International Journal of Wildland Fire 25(2), 200–212
doi: 10.1071/15091_AC

Supplementary material

Future burn probability in south-central British Columbia

Xianli Wang[A,E], *Marc-André Parisien*[B], *Stephen W. Taylor*[C], *Daniel D. B. Perrakis*[D], *John Little*[B] *and Mike D. Flannigan*[A]

[A]Department of Renewable Resources, University of Alberta, 751 General Service Building, Edmonton, AB T6G 2H1, Canada.

[B]Northern Forestry Centre, Canadian Forest Service, Natural Resources Canada, 5320 122nd Street, Edmonton, AB T6H 3S5, Canada.

[C]Pacific Forest Centre, Canadian Forest Service, Natural Resources Canada, 506 West Burnside Road, Victoria, BC V8Z 1M5, Canada.

[D]British Columbia Ministry of Forests, Lands and Natural Resource Operations, Wildfire Management Branch, 2957 Jutland Road, 2nd Floor, Building A, Victoria, BC V8W 9C1, Canada.

[E]Corresponding author. Email: xianli@ualberta.ca

Appendix S1. Modelling the ignition grids (fixed factor)

The ignition grids (Fig. S1) were built using a logistic regression modeling method (Scott *et al*. 2012; Parisien *et al*. 2013) applied to a 100 × 100-m^2-resolution raster data framework over the study area. The dependent variable was a binary vector of presumed fire ignition locations (i.e. presences) and 500 randomly chosen background points (i.e. absences) that did not overlap with the fire presences. The fire locations were obtained from a digital atlas of >3-ha fires that occurred during 1981–2010. When the fire origin was unknown, the centroid of the fire polygon was used. Three explanatory variables were used in both lightning- and human-caused models: elevation, topographic position index, which is an index of concavity (calculated using a 3-km window), and solar radiation, which is computed from aspect and slope. The two additional

variables were only used for the human-caused models as proxies for anthropogenic influence: the distance to roads and road density (calculated using a 25-km moving window).

The ignition grids were constructed using a stepwise process. First, we used a generalised additive model (GAM) regression model implemented in the *R* functions `gam` and `step.gam` of the `gam` package (Hastie 2013) to select the best predictor variables for each combination of season and fire cause. Non-significant predictor variables were excluded. Secondly, generalised linear models (GLMs) were constructed using the *R* function `'glm'` to obtain logistic regression models of ignition probability as a function of the best predictor variables and their quadratic terms. Finally, fire ignition grids were obtained using the `predict` function of the *`raster`* *R* package (Hijmans 2014) to apply the logistic models to the rasterised predictor variables.

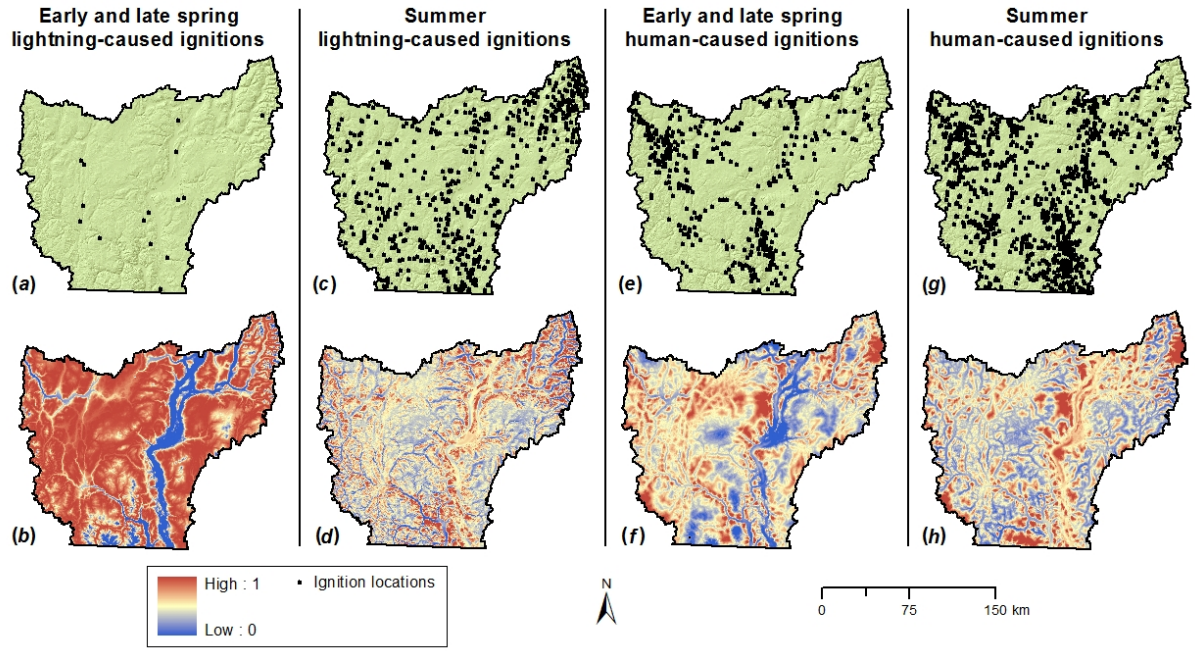

Fig. S1.1. Locations of >3-ha lightning- (*a* and *c*) and human-caused (*e* and *g*) fires (black dots) during the fire season. The lightning- (*b* and *d*) and human-caused (*f* and *h*) ignition grids used in

the Burn-P3 modeling. These grids represent the relative probability of ignition of fires ≥3 ha within a given combination of season and cause.

References

Hastie T (2013) gam: Generalized Additive Models. *R* package version 1.12. Available at http://CRAN.R-project.org/package=gam [Verified 26 November 2015]

Hijmans RJ (2014) raster: Geographic data analysis and modeling. *R* package version 2.3-12. http://CRAN.R-project.org/package=raster [Verified 26 November 2015]

Parisien M-A, Walker GR, Little JM, Simpson BN, Wang X, Perrakis DDB (2013) Considerations for modeling burn probability across landscapes with steep environmental gradients: an example from the Columbia Mountains, Canada. *Natural Hazards* **66**, 439–462.

R Core Team (2014) *R*: A language and environment for statistical computing. (R Foundation for Statistical Computing: Vienna, Austria) Available at http://www.R-project.org/ [Verified 26 November 2015]

Scott JH, Helmbrecht DJ, Parks SA, Miller C (2012) Quantifying the threat of unsuppressed wildfires reaching the adjacent wildland–urban interface on the Bridger–Teton National Forest, Wyoming, USA. *Fire Ecology* **8** (2), 125–142.

Appendix S2. The percentage cover of each Canadian Fire Behaviour Prediction System fuel type in the three fire zones, and the study area totals

Table S2.1. The percentage cover of each Fire Behavior Prediction System fuel type in the three fire zones

SAF, subalpine forest; GDF, grassland and dry forest; MTF, moist temperate forest

FBP fuel type[A]	Observed by fire zone				Baseline by fire zone				2080s by fire zone			
	SAF	GDF	MTF	All	SAF	GDF	MTF	All	SAF	GDF	MTF	All
C-2	4	0	0	2	0	0	0	0	0	0	0	0
C-3	60	12	39	36	88	54	27	66	28	14	22	21
C-4	1	0	2	1	0	0	0	0	0	0	0	0
C-5	1	1	29	4	4	1	67	11	50	13	51	35
C-7	16	49	9	30	0	27	1	11	15	55	22	32
D-1, 2	1	2	9	2	0	0	0	0	0	0	0	0
M-1, 2	1	2	5	2	0	0	0	0	0	0	0	0
S-1	2	1	1	1	0	0	0	0	0	0	0	0
O-1a	10	26	3	17	0	6	0	2	0	4	0	2

[A]C-2, Boreal spruce; C-3, mature jack or lodgepole pine; C-4, immature jack or lodgepole pine; C-5, red and white pine; C-7, ponderosa pine–Douglas-fir leafless; D-1, 2, aspen; M-1, 2, boreal mixedwood; S-1, jack or lodgepole pine slash; O-1a, matted grass.

Table S2.2. **The proportion of fires (%) (i.e. escaped fire rates) used in Burn-P3 simulations for the observed period by fire season, cause of ignition and fire zone**

SAF, subalpine forest; GDF, grassland and dry forest; MTF, moist temperate forest

	Escaped fire rate (%)					
Fire zone	Human			Lightning		
	Early spring	Late spring	Summer	Early spring	Late spring	Summer
SAF	0.4	1.34	9.64	0	0.25	10.66
GDF	9.14	10.8	35.21	0.07	0.47	10.26
MTF	0.44	1.16	3.73	0.04	0.36	6.03

Appendix S3. Modeling fuel type distribution in the baseline and 2080s time periods

Machine-learning methods were used to fit a bioclimatic envelope model (BEM) (Guisan and Zimmermann 2000) to the distribution of ecosystem units and a number of climatic variables in the observed period. The BEM was then used to project the baseline and 2080s ecosystem units by substituting climatic variables from the high CO_2 emission scenario (A2) of the Canadian global climate change model, CGCM3.2; A2 assumes that the concentration of CO_2 will double by the end of the 21st century, and temperature will increase by 2.0–5.4°C (ICPP 2007). The ecosystem units were then converted to Fire Behaviour Prediction (FBP) System fuel types (Forestry Canada Fire Danger Group 1992).

Methods

Ecosystem units and modeling extent

We considered an area much larger than the study area for the bioclimatic envelope modeling (48 to 52°N –123 to –117°W) to include more climatic variation, although model predictions were subsequently clipped to the study area. All variables were converted to 1-km^2-resolution grids in Lambert conformal conic (LCC) projection.

The finest-scale ecosystem units that have been mapped in the model extent, the 'variant' level of the British Columbia biogeoclimatic ecological classification (BEC) system (version four) (MSRM 2002) and 'level 4' of the USA ecoregion maps (EMGR 2007) were the dependent variable; there were a total of 105 ecosystem units. Areas of irrigated agriculture (non-fuels) were added from the Land Cover for Agricultural Regions database (Agriculture and Agri-Food Canada 2000).

Bioclimatic variables

Monthly maximum and minimum temperature and precipitation variables were used to calculate 20 biologically relevant and interpretable climate variables for both the baseline and 2080s periods (Table S3.1). These variables include growing season precipitation and temperature, dryness indices, various degree-days, frost-free period, dryness indices, temperature extremes and snowfall (Wang *et al*. 2012*a*). Monthly values for the baseline period were obtained from the 1-km-resolution ClimateWNA (Wang *et al*. 2012*b*) dataset that was generated using the Parameter Regression of Independent Slopes Model (PRISM Climate Group 2004) to interpolate observed climate normals between locations (Daly *et al*. 2000; Daly *et al*. 2002). Projected future climates were generated by overlaying interpolated 1-km-resolution modeled climate anomalies (between 1961–90 and 2071–2100 time periods) onto the 1961–90 data (Wang *et al*. 2012*b*).

Because topographic variations may also have significant impacts on BEM fits and predictions (Pearson and Dawson 2003; Coudun *et al*. 2006; Luoto and Heikkinen 2008), we also included radiation (RAD, computed from aspect and slope), slope (SLP) and topographic position index (TPI, an index of concavity, calculated using a 3-km window with a geographic information system (GIS) extension (http://www.jennessent.com/arcview/tpi.htm, accessed 26 November 2015) based on the digital elevation model (DEM)) in the model; topographic data were obtained from US Geological Survey (USGS), Earth Resources Observation Science (EROS).[1]

[1] http://edc.usgs.gov/products/elevation/gtopo30/gtopo30.html, accessed 20 May 2013.

Bioclimatic envelop modeling

The bioclimatic variables were used to construct an ecosystem unit BEM using a Random Forests technique (Breiman 2001) implemented in the R function '`randomForest`' (Liaw and Wiener 2002). In order to reduce the input data size and balance the prediction model, we randomly sampled 100 data points from each modeling unit (variant and level 4 for Canada and USA respectively). The out-of-bag (OOB) error rate was used to evaluate the goodness of fit. Within a fixed group of predictor variables, OOB varies with the number of simulated trees (ntree) (Peters *et al*. 2007). In order to obtain the 'optimal' model for the projection of ecosystems, we performed tests with various predictor variable combinations and ntree values, and used the model when OOB error rate is low and ntree is small. The final ecosystem BEM was used to generate baseline and 2080s ecosystem maps.

Fuels mapping

We created a 'crosswalk' table (Table S3.2) to convert the BEC variant and level 4 ecoregion units to FBP System fuel types based on their respective definitions (e.g. Meidinger and Pojar 1991) and expert knowledge. Because there are fewer FBP System fuel types than ecological units, the fuel types encompass many ecosystem units. Fuel type maps were obtained by applying the ecosystem-fuel type crosswalk table to the baseline and 2080s ecosystem maps. The projections were constrained by a rule that non-fuel areas remain non-fuel.

Model evaluation

The ecosystem unit BEM fitted the observed data reasonably well considering the coarse nature of the analysis (mean error rate = 31% for the 105 ecosystem units). The classification accuracy of the fuel types (Table S3.3), which was summarised from the confusion table of the

ecosystem BEM (see the summary by ecozone (Table S3.4)), showed higher prediction accuracy (hit rates) ranging between 83 and 92%. Both the baseline and 2080s ecosystem projections also qualitatively agree with the results for this region from an earlier study (Wang *et al*. 2012*a*) that project an increase in the bunchgrass and ponderosa zone at lower elevations (corresponding to our FBP fuel types 0-1a and C-7) and in the interior cedar hemlock zone at medium elevations (corresponding to our FBP C-5 fuel type). The cedar–hemlock vegetation complex is not explicitly defined as a fuel type in the Canadian Fire Behavior Prediction System, although Canadian fire behaviour specialists have determined that the fire behaviour in this vegetation type is similar to the C-5 fuel type. These evaluations suggested that the random forest (RF) projections were acceptable for our research objectives – to evaluate the effects of plausible changes in fuel conditions on burn probability.

However, it is important to note that the spatial patterns of fuels are simpler for the baseline than observed periods. This is because the observed fuels are strongly influenced by fine-scale anthropogenic land-use practices and natural disturbances (Fig. 2*a*) whereas the baseline fuels grid (Fig. 3) represents the expected fuel and vegetation pattern under broad-scale baseline climate conditions. The baseline fuels grid is also significantly different from that of the 2080s where most of the C-3 fuels in the baseline were replaced by C-5 (Fig. 3).

References

Agriculture and Agri-Food Canada (2000) Data specification: land cover for agricultural regions, ca. 2000. Available at http://www.agr.gc.ca/atlas/supportdocument_documentdesupport/circa2000Landcover/en/ [Verified 26 November 2015]

Breiman L (2001) Random forests. *Machine Learning* **45**, 5–32.

Coudun C, Gégout JC, Piedallu C, Rameau JC (2006) Soil nutritional factors improve plant species distribution models: an illustration with *Acer campestre* (L.) in France. *Journal of Biogeography* **33**, 1750–1763.

Daly C, Taylor GH, Gibson WP, Parzybok TW, Johnson GL, Pasteris PA (2000) High-quality spatial climate data sets for the United States and beyond. *Transactions of the Asae* **43**, 1957–1962.

Daly C, Gibson WP, Taylor GH, Johnson GL, Pasteris P (2002) A knowledge-based approach to the statistical mapping of climate. *Climate Research* **22**, 99–113.

EMGR (2007) Ecoregion maps and GIS resources. US Environmental Protection Agency, Western Ecology Division official website. (Corvallis, OR) Available at http://www.epa.gov/wed/pages/ecoregions.htm [Verified 26 November 2015]

Guisan A, Zimmermann NE (2000) Predictive habitat distribution models in ecology. *Ecological Modelling* **135**, 147–186.

IPCC (2007) Climate Change 2007: Synthesis report. Contribution of Working Groups I, II and III to the fourth assessment report of the Intergovernmental Panel on Climate Change. (Eds RK Pachauri, A Reisinger) (IPCC: Geneva, Switzerland)

Liaw A, Wiener M (2002) Classification and Regression by randomForest. *Rnews* **2**, 18–22.

Luoto M, Heikkinen RK (2008) Disregarding topographical heterogeneity biases species turnover assessments based on bioclimatic models. *Global Change Biology* **14**, 483–494.

Meidinger D, Pojar J (1991) Ecosystems of British Columbia. Special Report Series no. 6. (BC Ministry of Forests: Victoria, BC) Available at ttp://www.for.gov.bc.ca/HRE/becweb/resources/codes-standards/standards-species.html [Verified 26 November 2015]

MSRM (2002) Ministry of Sustainable Resource Management GIS data ftp site. Biogeoclimatic ecosystem classification coverage version 4. (Victoria, BC) Available at http://srmwww.gov.bc.ca/gis/arcftp.html

Pearson RG, Dawson TP (2003) Predicting the impacts of climate change on the distribution of species: are bioclimate envelope models useful? *Global Ecology and Biogeography* **12**, 361–371.

Peters J, De Baets B, Verhoest NEC, Samson R, Degroeve S, De Becker P, Huybrechts W (2007) Random forests as a tool for ecohydrological distribution modelling. Ecological modelling **207**, 304–318.

PRISM Climate Group (2004) PRISM Climate Data. Available at http://prism.oregonstate.edu [Verified 26 November 2015]

R Development Core Team (2010) *R*: A language and environment for statistical computing. (R Foundation for Statistical Computing: Vienna, Austria)

Wang T, Campbell EM, O'Neill GA, Aitken SN (2012*a*) Projecting future distributions of ecosystem climate niches: uncertainties and management applications. *Forest Ecology and Management* **279**, 128–140.

Wang T, Hamann A, Spittlehouse DL, Murdock TQ (2012*b*) ClimateWNA – High-resolution spatial climate data for western North America. *Journal of Applied Meteorology and Climatology* **51,** 16–29.

Table S3.1. Bioclimate variables, followed by abbreviations, used in the regression tree modelling

Elevation	elev	Mean annual precipitation	MAP	Hargreaves climatic moisture deficit	NEW_CMD
Radiation	rad	Mean summer[B] precipitation	MSP	Degree-days <0°C, chilling degree-days	DD01
Slope	slp	Mean winter[C] temperature	TAVG_WT	Degree-days >5°C, growing degree-days	DD51
Topographic index	tpi	Mean summer temperature	TAVG_SM	Extreme min. temperature over 30 years	EMT
Mean annual temperature	MAT	Winter precipitation	PPT_WT	No. of frost-free days	NFFD
Mean warmest month temperature (July)	MWMT	Summer precipitation	PPT_SM	Precipitation as snow	PAS
Mean coldest month temperature (January)	MCMT	Climatic moisture index	NEW_CMI	Hargreaves reference evaporation	E_REF
Continentality[A]	TD	Summer CMI	NEW_CMIJJA	Potential evapotranspiration	PET

[A]TD = MWMT – MCMT.
[B]Summer = June–August.
[C]Winter = December–February.

Table S3.2. Crosswalk between BC Biogeoclimatic subzones, US level 4 ecoregion units and FBP System fuel types

FBP System fuel type	BC biogeoclimatic subzones and US level 4 ecoregion units
C-3	BC: ESSFdc, ESSFdcp, ESSFdk, ESSFdv, ESSFdvp, ESSFmm, ESSFmmp, ESSFmw, ESSFmwp, ESSFvc, ESSFvcp, ESSFwc, ESSFwcp, ESSFwk, ESSFwm, ESSFwmp, ESSFxc, ESSFxcp, ESSFxv ,IDFdk, IDFdm, IDFmw, IDFun, IDFww
	US: 15x, 15y, 77d, 77g
C-5	BC: CDFmm, CWHdm, CWHds, CWHms, CWHvm, CWHvm, CWHxm , ICHmk, ICHmw, ICHvk, ICHwk, ICHmw, MHmm, MSdc, MSdk, MSdm, MSun, MSxk, MSxv, SBPSmk, SBPSxc, SBSdw, SBSmc, SBSmm, SBSun
	US: SA1, SA2, 2a, 2b, 2c, 2d, 2e, 2f, 15w, 77a, 77b
C-7	BC: ICHdk, ICHdw, ICHxw, IDFxh, IDFxm, IDFxw IDFxwa, IDFxwb, PPdh, PPxh
	US: 15g, 15r, 15u, 77e, 77f
O-1a	BC: BGxh, BGxw, BGxw
	US: 10a ,10d, 10m, 15s
Non-fuel	BC: A1 ATun ATunp
	US: 15h, 77c

Table S3.3. Classification accuracy matrix for the random forest model based on FBP System fuel types. Sensitivity represents out-of-bag classification accuracy

Predicted	Actual				Sensitivity
	C-3	C-5	C-7	O-1a	
C-3	10748	578	365	5	0.92
C-5	659	6449	55	7	0.90
C-7	373	65	3351	243	0.83
O-1a	5	1	225	2259	0.91

Table S3.4. Classification accuracy matrix summarised by BEC zone

BG, bunchgrass; CDF, coastal Douglas-fir; CWH, coastal western hemlock; ESSF, Engelmann spruce–subalpine fir; ICH, interior cedar–hemlock; IDF, interior Douglas-fir; MH, mountain hemlock; MS, montane spruce; PP, ponderosa pine; SBPS, sub-boreal pine–spruce; SBS, sub-boreal spruce

		Actual															Sensitivity
		10	15	2	77	BG	CDF	CWH	ESSF	ICH	IDF	MH	MS	PP	SBPS	SBS	
Predicted	10	775	31	0	23	8	0	0	0	0	0	0	0	3	0	0	0.92
	15	29	1851	0	0	2	0	0	18	38	16	0	13	17	0	0	0.93
	2	0	0	1479	11	0	12	2	0	0	0	0	0	0	0	0	0.98
	77	25	2	12	1561	5	0	22	18	0	18	9	8	8	0	0	0.92
	BG	1	2	0	0	1294	0	0	0	0	67	0	0	102	0	0	0.88
	CDF	0	0	1	0	0	188	4	0	0	0	0	0	0	0	0	0.97
	CWH	0	0	3	3	0	13	1603	19	0	56	93	10	0	0	0	0.89
	ESSF	0	5	0	25	0	0	12	4131	256	10	44	195	0	0	67	0.87
	ICH	0	23	0	0	0	0	0	272	2294	148	0	52	2	0	62	0.80
	IDF	0	17	0	8	88	0	37	2	144	3135	0	190	85	29	15	0.84
	MH	0	0	0	0	0	0	84	35	0	0	479	2	0	0	0	0.80
	MS	0	1	0	9	0	0	2	184	55	141	0	1276	0	30	9	0.75
	PP	0	3	0	2	95	0	0	0	3	84	0	0	551	0	0	0.75
	SBPS	0	0	0	0	0	0	0	2	3	25	0	19	0	519	32	0.87
	SBS	0	0	0	0	0	0	0	30	40	3	0	3	0	15	811	0.90

Appendix S4. Examples of projected changes in monthly average temperature and precipitation between baseline (1961-90) and 2080s (2071-2100) periods at representative weather stations in the three fire zones

Spring and summer temperatures are projected to increase by 3–4°C by the 2080s. Precipitation is projected to increase in spring and decrease in late summer (August). These temperature changes are close to the median values, as calculated for an ensemble of 30 GCM projections compiled by the Pacific Climate Impacts Consortium for this region (http://www.plan2adapt.ca/, accessed 18 February 2014) where the 30 members are produced by 15 different GCMs each using one run of the A2 and B1 emissions scenarios. These projected changes in climate drive the changes in fuels, fire weather ignitions in this study

Location		Average monthly temperature (°C)							Average monthly precipitation (mm)						
(Fire zone)		A	M	J	J	A	S	O	A	M	J	J	A	S	O
Lumby	1961–90	7.2	11.3	15.2	17.6	17.3	12.6	6.2	41.8	61.8	72.1	58.8	48.3	46.4	42.8
559 m	2070–2100	10.1	15.2	18.4	21.7	21.3	16.0	9.0	56.7	78.6	91.7	59	41.9	50.5	65.4
(MTF)	Δ	2.9	4.0	3.3	4.1	4.0	3.5	2.8	14.9	16.8	19.6	0.2	–6.4	4.1	22.6
Princeton	1961–90	6.4	10.7	14.8	17.6	17.5	12.8	6.6	18.1	23.4	29.5	28.6	25.6	21.5	20.5
701 m	2071–2100	9.7	14.0	17.7	22.0	21.8	16.9	9.4	19.5	31.7	40.8	27.7	19.3	26.9	30.7
(GDF)	Δ	3.3	3.3	2.9	4.4	4.3	4.1	2.8	1.4	8.3	11.3	–0.9	–6.3	5.4	10.2
Brenda Mines	1961–90	2.0	6.6	10.7	13.9	13.9	9.2	3.6	36.6	47.3	44.7	38.9	38.6	36.9	41.4
1520 m	2071–2100	5.2	10.0	13.5	17.2	18.2	13.2	6.5	45.8	68.5	68.5	57.5	33.6	41.6	62.1
(SAF)	Δ	3.2	3.4	2.8	3.3	4.3	4.1	2.9	9.2	21.2	23.8	18.6	–5.0	4.7	20.7

Appendix S5. Modelling the number of ignitions

Using a stepwise procedure, we fitted a generalised linear model to the annual number of fires >3 ha (S1) and fire weather variables (noon daily temperature, relative humidity, wind speed, precipitation in the previous 24 h, and the six codes or indexes of the FWI System) and their quadratic terms, recorded during 1987–2009; variables were averaged across 12 selected weather stations (see Fig. 2*c*) by fire season and for each summer month (June–August). Weather stations were selected that had continuous records, were distributed evenly across the study area, and covered all three fire zones; station elevations ranged between 472 and 1476 m with an average of 1013 m. The best predictions were obtained with a Poisson regression model with mean temperature and mean July drought code (DC) values as explanatory variables (variance explained = 53%; see Parks *et al*. 2012).

A bootstrap sampling approach was applied to the Poisson model predictions to generate data for the baseline and 2080s. We first randomly selected 12 locations (equivalent to the number of weather stations used for the observed period) from the 188-location dataset simulated with *BioSIM*, and then calculated the monthly mean temperature and DC values in July for each of the 30 years over all sampled weather stations. Second, we made 30 estimates of the annual ignition number using the Poisson predictive models. This procedure (drawing another 12 random locations) was repeated 1000 times, generating 1000 × 30 ignition numbers for each time period. These were incorporated into Burn-P3 as frequency distributions of the annual number of escaped fires.

References

Parks SA, Parisien M-A, Miller C (2012) Spatial bottom–up controls on fire likelihood vary across western North America. *Ecosphere* **3**, 1–20.

Appendix S6. Fire size (ha) distributions (kernel density curves, log-scale) obtained from Burn3 simulations for the baseline and 2080s periods, the latter modelled with changing Fuels, Weather, and Ignitions factors and their combinations (F, W, I, F × W, F × I, W × I, F × W × I)